JOURNAL OF MATERIALS SCIENCE 29 (1994) 5485–5490

Hydrogen effects on the ductile to brittle transition behaviour of 21-6-9 stainless steel

D. P. HARVEY II
Mechanics of Materials Branch, Naval Research Laboratory, Washington, DC 20375, USA
J. B. TERRELL
Reynolds Metals Company, Richmond, VA 23221, USA
T. S. SUDARSHAN
Materials Modification, Inc., Fairfax, VA 22031, USA

Charpy V-notched impact test studies on 21-6-9 austenitic stainless steel at 293 and 77 K demonstrated that hydrogen charging promoted the formation of larger microvoids at 293 K, promoted the formation of facets at 77 K, and reduced the energy absorbed by the material at both temperatures. These observations suggest that the role of hydrogen in the impact behaviour of this material is to enhance whatever crack-growth mechanism is operating at a given temperature. Further, the observation that embrittlement exists even at liquid nitrogen temperatures indicates that little or no localized rearrangement of hydrogen during the test is required or that relatively high strain-rate effects on hydrogen embrittlement need not be necessarily attributed to enhanced transport of hydrogen atmospheres by mobile dislocations. The data presented in this paper are consistent with a model in which the mechanism of hydrogen embrittlement is affected by the extent of plastic deformation.

1. Introduction

Previous investigations have established the behaviour of conventional Fe–Cr–Ni stainless steels in hydrogen environments [1–6] and, although susceptible to hydrogen embrittlement, these alloys appear adequate for most hydrogen service. However, most of this work has been principally concerned with tensile properties and crack-growth behaviour. These studies have also shown that the tendency for embrittlement generally increases as the strain rate is decreased in hydrogen-charged specimens and that a ductility minimum can be observed at 220 K with no effect being observed around 77 K. Despite the recognition of the importance of strain rate in hydrogen and low-temperature environments, little work has addressed the role of hydrogen on the impact behaviour of stainless steels. It is often assumed by designers that austenitic stainless steels (predominantly Fe–Cr–Ni) do not exhibit a ductile-to-brittle transition, although such behaviour has been demonstrated in Fe–Cr–Mn steels. Work done over the last decade or so, however, has clearly demonstrated that several Fe–Cr–Ni austenitic steels [7–10] are indeed susceptible to hydrogen effects even at liquid nitrogen temperatures (77 K). It is essential, therefore, that if such steels are to be considered for low-temperature structural applications that their tendency for brittle fracture be investigated. Hydrogen is known to have a deleterious effect on the fracture behaviour of most ferrous alloys: however, there is a considerable degree of disagreement about the overall mechanism for embrittlement. Previous studies [11–15] have associated embrittlement with the interaction of hydrogen with grain-boundary impurities, plastic deformation processes, dislocations, deformation and martensite formation, stress gradients, interfaces and voids. Many of the suggested models require the redistribution of hydrogen during the test, resulting either in localized high concentrations or interaction with some microstructural feature produced during the test. At slow strain rates and at ambient temperatures, dislocation transport may be possible. However, impact testing strain rates are much higher than those used for tensile tests. These high strain rates coupled with low temperatures preclude any large-scale redistribution of hydrogen during testing, considering the low diffusivity of hydrogen in austenite at 77 K (10^{-43} $m^2 s^{-1}$).

2. Experimental procedure

The test specimens for these impact studies were machined from cross-rolled plate stock of Type 21-6-9 stainless steel. The composition of the test material is given in Table I. Room-temperature tensile properties of the test material are given in Table II. Modified Charpy V-notch specimens were machined according to ASTM E 23 A specifications from the stainless steel plate and charged with gaseous hydrogen. Hydrogen charging of the specimens was achieved by exposing the specimens to hydrogen gas at either 13.8 or 138 MPa in an autoclave maintained at 573 K for 45

0022–2461

TABLE I Composition (wt%) of 21-6-9 stainless steel test material

C	0.04
Mn	8.80
Si	0.32
P	0.017
S	0.013
Cr	19.34
Ni	5.89
N	0.29
O	0.007
Fe	Balance

TABLE II Room-temperature, quasi-static tensile properties of 21-6-9 stainless steel

Yield stress (MPa)	568
Ultimate stress (MPa)	775
Elongation (%)	34.4
Reduction in area (%)	74.9

days. No attempts were made to measure the hydrogen content in these specimens. The exposed specimens were then removed from the autoclave and stored at 273 K until they were tested. Uncharged control specimens were also heated at 573 K for 45 days in order to eliminate thermal treatment effects as an experimental variable. Impact tests were performed using an instrumented impact machine on the hydrogen-charged and the uncharged specimens at 293 and 77 K. Oscilloscope readings of absorbed energy and load versus time were photographed for each test and subsequently digitized on to a computer. Fractographic observations were made on selected specimens to determine the effects on hydrogen exposure on the fracture process.

3. Results

The peak loads and absorbed energy for all of the tests are summarized in Table III. The load versus time traces are schematically depicted in Fig 1a–c and 2a and b. A comparison of uncharged specimens with hydrogen-charged specimens led to the following general observations.

(a) A decrease in temperature is accompanied by an increase in peak load and a decrease in energy absorbed. The decrease in absorbed energy with temperature is most severe at the highest level of hydrogen charging.

TABLE III Results of 21-6-9 stainless steel impact tests

Test temperature (K)	Hydrogen-charging condition (MPa)	Energy absorbed (J)	Peak load (kN)	Uncharged energy %
293	0	359	23.1	100
293	13.8	336	23.1	94
293	138	295	23.1	82
77	0	54	31.1	100
77	13.8	51	32.7	94
77	138	37	31.6	69

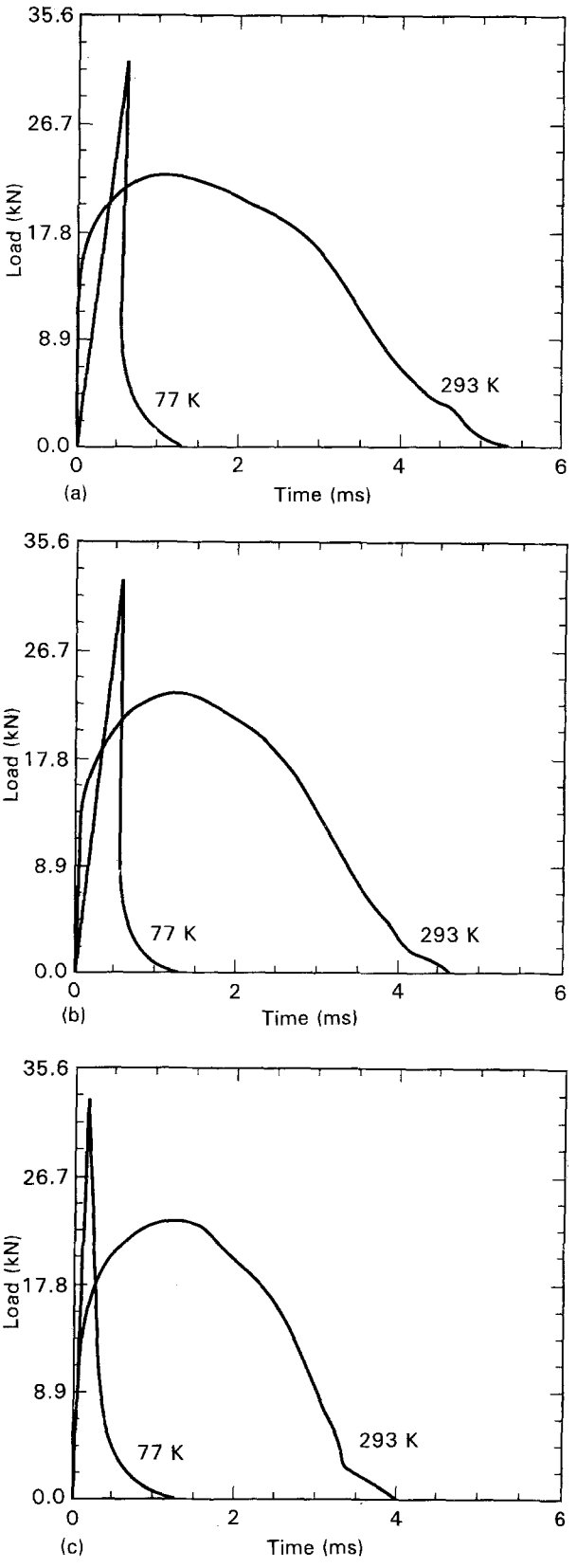

Figure 1 Load–time traces of (a) uncharged specimens, (b) specimens charged at 13.8 MPa hydrogen, and (c) specimens charged at 138 MPa hydrogen.

(b) Hydrogen charging by itself causes a decrease in energy absorbed. These reductions are more severe at 77 K than at 293 K.

(c) Hydrogen charging displaces the load–time traces to the left of the uncharged specimens at both temperatures (Fig. 2).

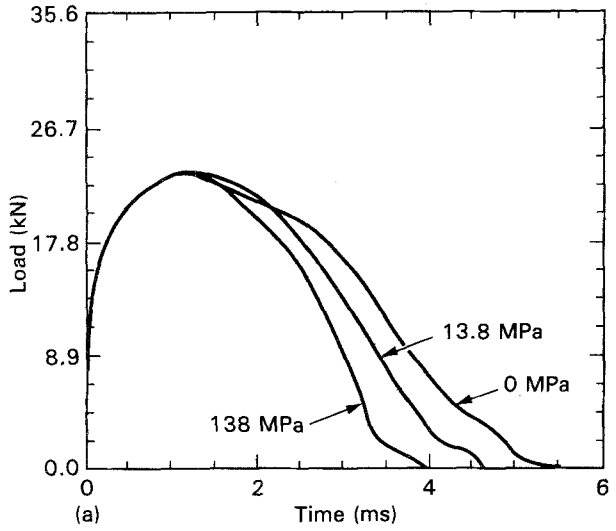

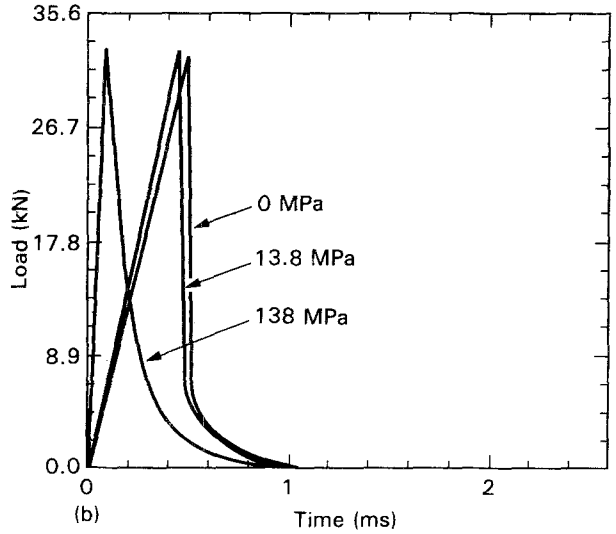

Figure 2 Load–time traces of specimens tested at (a) 293 K and (b) 77 K, all hydrogen charging levels.

The fracture surfaces of all specimens showed regions of ductile rupture, although frequently a heterogeneous distribution of microvoid sizes was present. The microvoids in the specimens tested at 293 K increased in size as hydrogen content increased as shown in Figs 3 and 4 which show the fracture surfaces of the specimens exposed to 0 and 138 MPa hydrogen, respectively. The fracture surfaces of the specimens tested at 77 K exhibited both dimples and facets. The tendency towards brittle fracture increased with hydrogen charging as shown in Figs 5 and 6 which show the fracture surfaces of the specimens exposed to 13.8 and 138 MPa hydrogen, respectively. The specimens tested at 77 K and charged at 138 MPa hydrogen, also exhibited secondary cracking as shown in Fig. 7. A summary of the observed fracture features is provided in Table IV.

4. Discussion

The impact tests performed on uncharged specimens at room temperature yielded the highest values for absorbed energy in this study. Lowering the test temperature to 77 K from 293 K severely decreased the

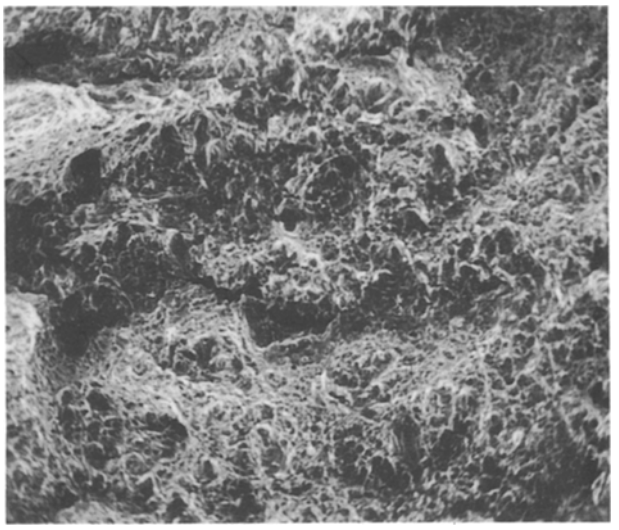

Figure 3 Fracture surface of uncharged specimen tested at 293 K, X 300.

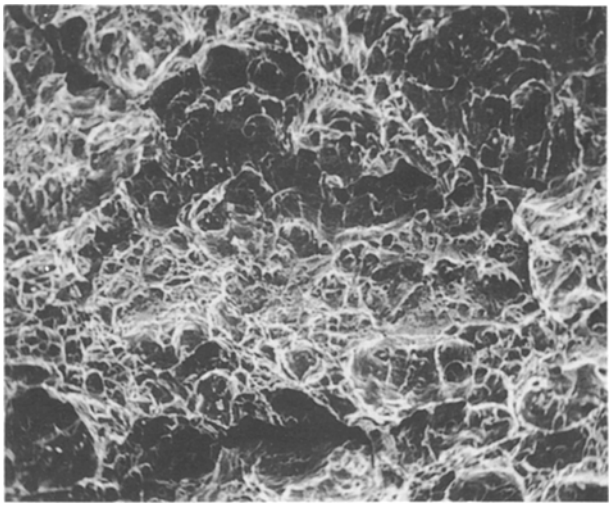

Figure 4 Fracture surface of specimen charged at 138 MPa hydrogen and tested at 293 K, X 300.

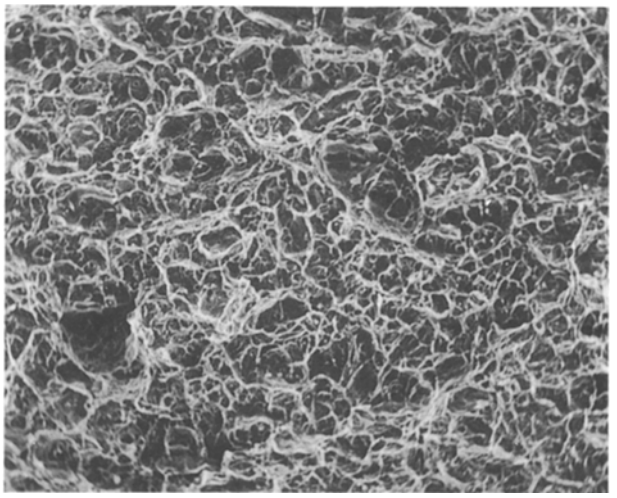

Figure 5 Fracture surface of specimen charged at 13.8 MPa hydrogen and tested at 77 K, X 300.

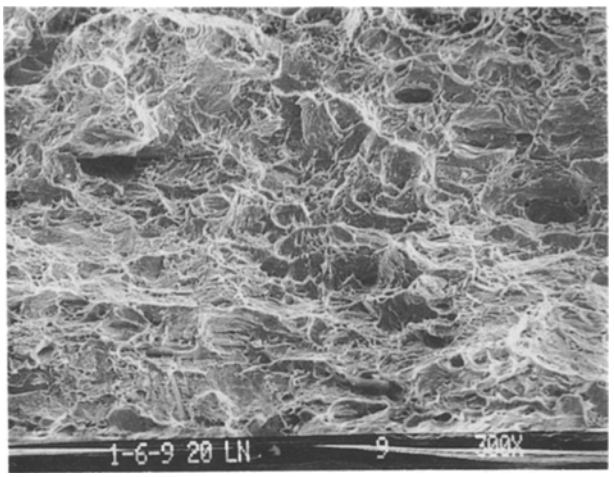

Figure 6 Fracture surface of specimen charged at 138 MPa hydrogen and tested at 77 K, X 300.

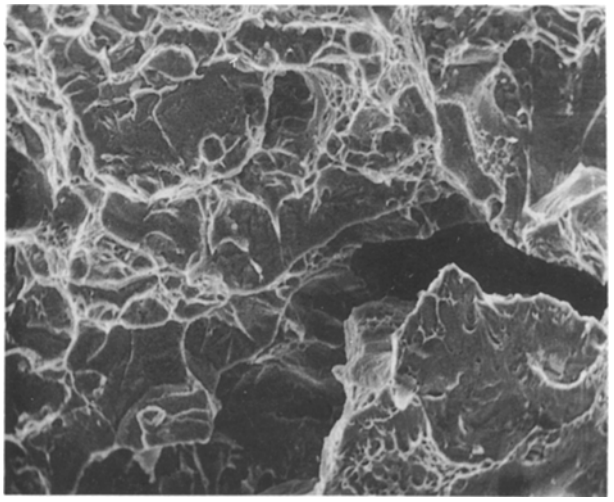

Figure 7 Secondary cracking observed in specimen charged at 138 MPa hydrogen and tested at 77 K, X 1000.

TABLE IV Fracture features observed in 21-6-9 stainless steel impact tests

Test Temperature (K)	Hydrogen-charging condition (MPa)	Fracture features
293	0	Dimples
293	13.8	Larger dimples
293	138	Still larger dimples
77	0	Dimples and facets
77	13.8	Dimples and more facets
77	138	Dimples and still more facets, secondary cracking

energy absorbed by the material. A change in fracture mode from microvoid coalescence to mixed ductile and brittle fracture was observed at all hydrogen charging levels with a decrease in test temperature. The change in fracture mode and decrease in absorbed energy are due to the existence of a ductile-to-brittle transition in this alloy. The existence of faceted fracture is not simply a hydrogen-induced effect; however, as the degree of hydrogen charging increased at 77 K, more faceted fracture resulted, supporting the embrittlement hypothesis that hydrogen absorption lowers the strength of interfaces in the austenitic lattice. The decrease in absorbed energy with a decrease in temperature was also more severe at the highest level of hydrogen charging. This observation suggests that sufficiently high levels of absorbed hydrogen changes the ductile-to-brittle transition behaviour of the test material.

As the level of hydrogen charging increased, the energy absorbed by the specimens decreased at both 293 and 77 K. Many models of hydrogen embrittlement require the redistribution of hydrogen during dynamic testing for the embrittlement process to be operative. Dislocation transport of hydrogen has been proposed as the redistribution mechanism under conditions of dynamic testing while the strain-rate dependence of hydrogen embrittlement has been used as experimental support for the role of dislocation transport in hydrogen embrittlement processes. However, the observation of hydrogen embrittlement at 77 K in this and previous studies [7–9] suggest that long-range hydrogen redistribution during testing is not a necessary prerequisite for hydrogen-induced degradation of the mechanical properties of austenitic stainless steels. This conclusion is emphasized by noting that the diffusivity of hydrogen in austenite at 77 K is approximately 10^{-43} $m^2 s^{-1}$. When hydrogen diffusivity is so low at 77 K the maximum redistribution distance that is possible during testing is calculated to be far less than 0.1 nm (one jump distance). Under these low-temperature conditions, test-induced redistribution is virtually impossible. Thus, even if dislocation transport greatly increases the diffusivity, no significant long-range redistribution of hydrogen could occur in the limited time spans required for impact fracture tests. Therefore, this single observation provides strong evidence that the strain-rate dependence of hydrogen embrittlement in dynamic tests need not necessarily be rationalized solely through dislocation transport arguments, particularly at low temperatures. Other effects that may influence such embrittlement are orientation and/or interfacial strengths.

The instrumented impact machine has been used previously by several investigators to study the dynamic fracture behaviour of steels [16–18] and, more recently, of stainless steels [7–9]. The load–time and the energy–time traces can provide detailed information on the characteristics of the fracture processes during dynamic loading. Considering the room-temperature load–time traces (Fig. 2a), it is observed that until the maximum load is reached, hydrogen exerts a minimal effect on the properties of the material. However, after the maximum load is reached, the load–time trace is shifted to the left and the tearing slope becomes steeper with hydrogen charging. Because the observed changes in the load–time traces do not occur until after the peak load, this suggests that hydrogen is primarily affecting crack growth rather than crack nucleation in the specimens tested at ambient temperatures. The specimens tested at 293 K

failed by ductile rupture at all hydrogen charging levels. Ductile fracture is a result of the nucleation, growth and link-up of microvoids; either or all of these steps may be affected by hydrogen [19, 20]. The increase in the size of the dimples on the fracture surface with hydrogen charging at 293 K further suggest that hydrogen is affecting the growth of microvoids in these specimens by increasing the plasticity of ligaments between microvoids [21]. Hydrogen-enhanced plasticity was first proposed by Beachem [22] and supported by subsequent observations [19, 23–28]. It was observed that hydrogen enhanced dislocation motion and multiplication in the early stages of deformation and resulted in the formation of dislocation tangles [23, 27]. Although the dislocation motion was enhanced, it was also more localized [24]. The resulting dislocation structures are not changed by the presence of hydrogen [25], but the critical strain for the various stages of fracture are reduced by hydrogen [28]. This mechanism is consistent with the steeper drop in load observed with hydrogen charging at 293 K.

The load–time traces of the specimens tested at 77 K also show a shift to the left with hydrogen charging (Fig. 3b); however, in this case the shift occurs prior to as well as after the maximum load. This is a macroscopic result of the secondary cracking observed through fractography (Fig. 7). The energy required for nucleation of cracks in the specimens tested at 77 K with hydrogen charging is less than that for the uncharged specimens. This is evinced by the observed decrease in absorbed energy values and the presence of secondary cracking in the hydrogen-charged specimens tested at 77 K. When the impact hammer strikes a specimen, a certain amount of energy is available for the nucleation of cracks. In general, the energy required to separate interfaces in a material that exhibits a ductile-to-brittle transition temperature is greater at higher temperatures (293 K and above) than at lower temperatures. In this study, in the specimens charged at 138 MPa hydrogen and tested at 77 K, the available energy was sufficient to separate simultaneously several interfaces near the notched region which resulted in the creation of multiple cracks. This phenomenon of multiple initiation led to the growth of several of these cracks which was manifested in the form of the secondary cracks observed in the hydrogen-charged specimens tested at 77 K. As the impact process continued, all of these cracks coalesced with the most dominant crack front and resulted in final failure. The brittle fracture observed in the specimens tested at 77 K can be rationalized by the reduced strength of various interfaces due to the presence of lower temperature and/or the segregation of hydrogen to these interfaces. The degree of damage created by hydrogen or temperature on the interfacial strength of a given alloy are in competition with one another. The results also suggest that the environment (hydrogen or temperature) which dominates at a particular temperature is that which produces the greatest decrease in impact properties. The use of two different sets of specimens at the same temperature level (with and without hydrogen) also facilitates the separation of temperature effects and hydrogen effects. It is observed that at lower temperatures, the hydrogen effect is masked by the temperature effect on the impact properties of the test material. The combined presence of hydrogen and low temperatures may contribute synergistically to the increased ease for multiple initiation in the hydrogen-charged samples tested at low temperatures and is possibly manifested in this study in the form of a shift in the peak-load curve towards lower temperatures. These results can be sufficiently rationalized through a model for embrittlement that involves interfacial energies associated with separation. In such a model, it is hypothesized that temperature and hydrogen can create similar effects in a material. Support for this model is derived from other recent studies [10, 17, 18, 29–31] which showed that slip bands, twin boundaries, inclusions and grain boundaries all show different degrees of susceptibility to hydrogen embrittlement. Exposure of the specimens to hydrogen gas allows its segregation to several interfaces in the material. In this particular case, the hydrogen accumulation along the grain boundaries lowered the interfacial strengths thereby facilitating decohesion. Such a model is also consistent with the secondary cracking observed in the environmentally degraded specimens.

Although hydrogen charging did not induce a change in fracture mode from MVC to brittle fracture at either test temperature, it did affect the fracture mode operating at a given temperature. The amount of plasticity occurring at the crack tip was determined primarily by test temperature, as indicated by the rise in the peak load sustained by the specimens tested at 77 K. When the fracture mode was ductile (293 K), hydrogen enhanced crack growth by affecting microvoid growth as evinced by an increase in microvoid size and a steeper drop in load. When the fracture mode was more brittle (77 K), hydrogen lowered interfacial strengths, as indicated by an increase in faceted fracture and secondary cracking. Changes in fracture mode from microvoid coalescence to quasi-cleavage to intergranular in the hydrogen-assisted cracking of wedge-loaded steel specimens have been observed in previous studies [22]. These changes were attributed to the decrease in the stress intensity at the crack tip as the crack grew which in turn decreased the size of the plastic zone. The model proposed to explain these changes in fracture mode suggested that hydrogen aids whatever deformation processes a given combination of microstructure and applied stress intensity will allow. The results of this study are consistent with such a model.

5. Conclusions

1. Hydrogen charging affects the ductile-to-brittle transition behaviour of 21-6-9 stainless steel by reducing the energy absorbed by the material and by enhancing brittle fracture at low temperatures thus shifting the ductile-to-brittle transition temperature to the right (to higher temperatures).

2. Long-range internal redistribution of hydrogen is not a necessary prerequisite for the embrittlement of

21-6-9 stainless steel under conditions of dynamic loading.

3. The role of hydrogen in the impact behaviour of 21-6-9 stainless steel is that of enhancing the crack-growth mechanism operating at a given temperature. At 293 K, hydrogen-enhanced plasticity is manifested by a steeper drop in load and the formation of larger microvoids. At 77 K, the lowering of interfacial strengths by hydrogen is manifested by an increase in faceted fracture and secondary cracking.

Acknowledgements

The authors thank Dr M. R. Louthan Jr. for many enlightening discussions. His contributions over the years have stimulated our interest in environmental effects on metals and are gratefully acknowledged.

References

1. D. ELIEZER, in "Hydrogen in Metals", edited by A. W. Thompson and I. M. Bernstein (TMS-AIME, Warrendale, PA, 1983) p. 565.
2. D. NEJEM, M. HABASHI, J. GALLAND, S. TALBOT-BESNARD and P. AZOU, *ibid.*, p. 555.
3. B. C. ODEGARD Jr. and A. J. WEST, *ibid.*, p. 597.
4. J. A. DONOVAN, *Met. Trans.* **7A** (1976) 145.
5. A. J. WEST and M. R. LOUTHAN Jr, *ibid.* **10A** (1979) 1675.
6. G. R. CASKEY, in "Hydrogen Degradation of Ferrous Alloys", edited by R. A. Oriani, J. P. Hirth and M. Smialowski (1985) p. 822.
7. T. A. PLACE, T. S. SUDARSHAN, C. K. WATERS and M. R. LOUTHAN Jr, in "Fractography of Modern Engineering Materials", edited by J. E. Masters and J. J. Au, ASTM STP 948 (American Society for Testing and Materials, Philadelphia, PA, 1986) p. 350.
8. J. M. HYZAK, D. E. RAWL Jr. and M. R. LOUTHAN Jr, *Scripta Metall.* **15** (1981) 937.
9. J. A. WAGNER, MS thesis, Virginia Polytechnic Institute and State University (1983).
10. K. L. ROHR, MS thesis, Virginia Polytechnic Institute and State University (1986).
11. R. D. KANE and B. J. BERKOWITZ, *Corrosion* **36** (1980) 29.
12. H. HANNINEN and T. HAKKARAINEN, *Met. Trans.* **10A** (1979) 1196.
13. N. SRIDHAR, J. A. KARGOL and N. F. FIORE, *Scripta Metall.* **14** (1980) 225.
14. G. H. KOCK, *Corrosion* **35** (1979) 73.
15. C. L. BRIANT, *Met. Trans.* **10A** (1979) 181.
16. K. N. MURTY, N. K. RAO and H. KRISHNAN, *Eng. Fract. Mech.* **18** (1983) 1173.
17. K. E. STAHLKOPF, R. E. SMITH, W. L. SERVER and R. A. WULLAERT, in "Cracks and Fracture", edited by J. L. Swedlew and M. L. Williams, ASTM STP 601 (American Society for Testing and Materials, Philadelphia, PA, 1976) p. 291.
18. J. B. TERRELL, T. S. SUDARSHAN and K. L. ROHR, *J. Heat Treat.* **5** (1987) 21.
19. R. GARBER, I. M. BERNSTEIN and A. W. THOMPSON, *Scripta Metall.* **10** (1976) 341.
20. *Idem, Met. Trans.* **12A** (1981) 225.
21. A. W. THOMPSON, *ibid.* **10A** (1979) 727.
22. C. D. BEACHEM, *ibid.* **3A** (1972) 437.
23. T. TABATA and H. K. BIRNBAUM, *Scripta Metall.* **17** (1983), 947.
24. *Idem, ibid.* **18** (1984) 231.
25. I. M. ROBERTSON and H. K. BIRNBAUM, *ibid.* **18** (1984) 269.
26. T. MATSUMOTO, J. EASTMAN and H. K. BIRNBAUM, *ibid.* **15** (1981) 1033.
27. J. EASTMAN, T. MATSUMOTO, N. MARITA, F. HEUBAUM and H. K. BIRNBAUM, in "Hydrogen Effects in Metals", edited by A. W. Thompson and I. M. Bernstein (TMS-AIME, Warrendale, PA, 1981) p. 397.
28. T. D. LEE, T. GOLDENBERG and J. P. HIRTH, *Met. Trans.* **10A** (1979) 199.
29. N. C. PRUITT Jr, T. S. SUDARSHAN and M. R. LOUTHAN Jr, *J. Mater. Eng.* **10** (1988) 99.
30. R. C. WASIELEWSKI, MS thesis, Virginia Polytechnic Institute and State University (1983).
31. P. SADLER, N. C. PRUITT Jr, T. S. SUDARSHAN and M. R. LOUTHAN Jr, *J. Mater. Eng.* **9** (1987), 151.

Received 17 August 1992
and accepted 14 September 1993